REGULAR ARTICLE

blood advances

Distribution and clinical impact of molecular subtypes with dark zone signature of DLBCL in a Japanese real-world study

Tomohiro Urata,[1-3] Yusuke Naoi,[1-3] Aixiang Jiang,[4] Merrill Boyle,[4] Kazutaka Sunami,[5] Toshi Imai,[6] Yuichiro Nawa,[7] Yasushi Hiramatsu,[8] Kazuhiko Yamamoto,[9] Soichiro Fujii,[10] Isao Yoshida,[11] Tomofumi Yano,[12] Ryota Chijimatsu,[3] Hiroyuki Murakami,[1-3] Kazuhiro Ikeuchi,[1-3] Hiroki Kobayashi,[1-3] Katsuma Tani,[1-3] Hideki Ujiie,[3] Hirofumi Inoue,[13] Shuta Tomida,[3] Akira Yamamoto,[2] Takumi Kondo,[2] Hideaki Fujiwara,[2] Noboru Asada,[2] Hisakazu Nishimori,[2] Keiko Fujii,[2] Nobuharu Fujii,[2] Ken-ichi Matsuoka,[2] Keisuke Sawada,[14] Shuji Momose,[14] Jun-ichi Tamaru,[14] Asami Nishikori,[15] Yasuharu Sato,[15] Tadashi Yoshino,[16] Yoshinobu Maeda,[1,2] David W. Scott,[4] and Daisuke Ennishi[2,3]

[1]Department of Hematology, Oncology and Respiratory Medicine, Okayama University Graduate School of Medicine, Dentistry and Pharmaceutical Sciences, Okayama, Japan; [2]Department of Hematology and Oncology and [3]Center for Comprehensive Genomic Medicine, Okayama University Hospital, Okayama, Japan; [4]British Columbia Cancer, Centre for Lymphoid Cancer, Vancouver, BC, Canada; [5]Department of Hematology, NHO Okayama Medical Center, Okayama, Japan; [6]Department of Hematology and Blood Transfusion, Kochi Health Sciences Center, Kochi, Japan; [7]Division of Hematology, Ehime Prefectural Central Hospital, Matsuyama, Japan; [8]Department of Hematology and Oncology, Japanese Red Cross Society Himeji Hospital, Hyogo, Japan; [9]Department of Hematology and Oncology, Okayama City Hospital, Okayama, Japan; [10]Department of Hematology, Japanese Red Cross Okayama Hospital, Okayama, Japan; [11]Department of Hematologic Oncology, NHO Shikoku Cancer Center, Matsuyama, Japan; [12]Department of Internal Medicine, Okayama Rosai Hospital, Okayama, Japan; [13]Clinical Genomic Medicine, Okayama University Graduate School of Medicine, Dentistry, and Pharmaceutical Science, Okayama, Japan; [14]Department of Pathology, Saitama Medical Center, Saitama Medical University, Saitama, Japan; [15]Department of Molecular Hematopathology, Okayama University Graduate School of Health Sciences, Okayama, Japan; and [16]Department of Pathology, Okayama University, Okayama, Japan

Key Points

- ABC-DLBCL is enriched in Japanese DLBCL.
- DLBCL90 is a robust biomarker that is consistent across geographical areas.

The distribution and clinical impact of cell-of-origin (COO) subtypes of diffuse large B-cell lymphoma (DLBCL) outside Western countries remain unknown. Recent literature also suggests that there is an additional COO subtype associated with the germinal center dark zone (DZ) that warrants wider validation to generalize clinical relevance. Here, we assembled a cohort of Japanese patients with untreated DLBCL and determined the refined COO subtypes, which include the DZ signature (DZsig), using the NanoString DLBCL90 assay. To compare the distribution and clinical characteristics of the molecular subtypes, we used a data set from the cohort of British Columbia Cancer (BCC) (n = 804). Through the 1050 patient samples on which DLBCL90 assay was successfully performed in our cohort, 35%, 45%, and 6% of patients were identified to have germinal center B-cell–like (GCB) DLBCL, activated B-cell–like (ABC) DLBCL, and DZsig-positive ($DZsig^{pos}$) DLBCL, respectively, with the highest prevalence of ABC-DLBCL, differing significantly from the BCC result ($P < .001$). GCB-DLBCL, ABC-DLBCL, and $DZsig^{pos}$-DLBCL were associated with 2-year overall survival rates of 88%, 75%, and 66%, respectively ($P < .0001$), with patients with $DZsig^{pos}$-DLBCL having the poorest prognosis. In contrast, GCB-DLBCL without DZsig showed excellent outcomes after rituximab-containing immunochemotherapy. $DZsig^{pos}$-DLBCL was associated with the significant enrichment of tumors with CD10 expression, concurrent MYC/BCL2 expression, and depletion of microenvironmental components (all, $P < .05$). These results provide evidence of the distinct distribution of clinically relevant molecular subtypes in Japanese DLBCL and that refined COO, as measured by the DLBCL90 assay, is a robust prognostic biomarker that is consistent across geographical areas.

Submitted 12 April 2023; accepted 24 July 2023; prepublished online on *Blood Advances* First Edition 8 August 2023. https://doi.org/10.1182/bloodadvances.2023010402.

Data are available on request from the corresponding author, Daisuke Ennishi (daisukeennishi@okayama-u.ac.jp).

The full-text version of this article contains a data supplement.

© 2023 by The American Society of Hematology. Licensed under Creative Commons Attribution-NonCommercial-NoDerivatives 4.0 International (CC BY-NC-ND 4.0), permitting only noncommercial, nonderivative use with attribution. All other rights reserved.

Introduction

Diffuse large B-cell lymphoma (DLBCL), the most common type of lymphoma, has a heterogeneous and complex biology. DLBCL is divided into 2 molecular subtypes, with distinct biological and clinical characteristics, as revealed through the cell-of-origin (COO), based on gene expression profiling; germinal center B-cell-like DLBCL (GCB-DLBCL), and activated B-cell-like DLBCL (ABC-DLBCL).[1-3] The molecular subtyping of COO has been translated into immunohistochemistry (IHC)-based algorithms[4-7]; however, from 10% to 50% of these malignancies are misclassified based on the gene expression profiling–based COO classification, which is considered the gold standard,[6,8,9] contributing to a lower reproducibility of the prognostic significance.[9,10]

In addition, recent studies have developed gene expression signatures, the double-hit (DHIT) signature and the molecular high-grade signature, which can identify high-grade B-cell lymphoma with *MYC* and *BCL2* rearrangements (HGBL-DH-*BCL2*) as well as high-risk GCB-DLBCL with a similar gene expression profile.[11,12] These studies show that both gene expression signatures identify tumors with a distinct COO derived from the germinal center dark zone (DZ), which was supported by recent single-cell transcriptomic analyses.[13] The DHIT signature was also translated into an assay (DLBCL90) applicable to routine formalin-fixed paraffin-embedded (FFPE) tissues, which can be widely used in clinical practice.[11,14] Notably, a recent large-scale study using the DLBCL90 assay has shown that the DHIT signature identified a subgroup with the poorest prognosis that was expressed in all evaluated tumors of Burkitt lymphoma, an archetypical DZ lymphoma. Reflecting these findings, the DHIT signature was renamed as DZ signature (DZsig) and can be considered a refinement of the COO classification.[15]

These efforts have significantly contributed to the advancement of the molecular classification of DLBCL; however, data were derived from countries in North America and Europe, and the distribution of the molecular subtypes in other geographical regions remains unknown. Herein, we present the results of a molecular characterization based on the DLBCL90 assay in 1050 Japanese patients with DLBCL treated with rituximab-containing immunochemotherapy.

Patients and methods

Patient cohort

This study's patient cohort comprised 1576 patients who were consecutively diagnosed with de novo DLBCL, not otherwise specified, or HGBCL-DH with DLBCL morphology and treated with rituximab-containing immunochemotherapies between 2008 and 2018 at 9 institutions included in the Okayama Hematology Study Group. The 9institutions were all located in the Western part of Japan; Okayama University Hospital, National Hospital Organization (NHO) Okayama Medical center, Okayama City Hospital, Red Cross Okayama Hospital, Okayama Rosai Hospital (Okayama, Okayama), the Kochi Health Sciences Center (Kochi, Kochi), Ehime Prefectural Central Hospital, NHO Shikoku Cancer Center (Matsuyama, Ehime), and the Japanese Red Cross Society Himeji Hospital (Himeji, Hyogo). This study was reviewed and approved by ethics committee at participating institutions in accordance with the Declaration of Helsinki.

The study cohort also included patients meeting the following criteria: aged ≥18 years; treated with curative intent with rituximab, cyclophosphamide, doxorubicin, vincristine, and prednisone (R-CHOP) or R-CHOP–like immunochemotherapy for at least 1 cycle (median, 6; range, 1-8 cycles); and with available complete clinical and laboratory data. We permitted adding central nervous system relapse prophylaxis, such as high-dose IV methotrexate or intrathecal chemotherapy, if necessary, to the aforementioned standard chemotherapies. We excluded patients receiving intensified regimens: rituximab, cyclophosphamide, vincristine, doxorubicin, and dexamethasone (n = 19); rituximab, high-dose methotrexate, and cytarabine (n = 2); rituximab, dexamethasone, etoposide, ifosfamide, and carboplatin (n = 2); cyclophosphamide, cytarabine, etoposide, dexamethasone, and rituximab (n = 1); rituximab, ifosfamide, dexamethasone, etoposide, and cytarabine (n = 1); or rituximab, mitoxantrone, etoposide, and prednisolone (n = 1). Patients were excluded if they had primary mediastinal large B-cell lymphoma, primary central nervous system lymphoma, a history of an indolent lymphoma, history of intake of immune suppressors such as methotrexate, or positive HIV serology results. All tissues were reviewed by expert hematopathologists (Y.S. and Y.N.) to confirm the diagnosis.[16]

For the comparison of the distribution in refined COO subtypes (including DZsig) between Japanese and Western patients with DLBCL, we used population-based registry data from the British Colombia Cancer (BCC) study of 804 patients diagnosed with de novo DLBCL, 629 of whom were treated with R-CHOP.[15] Molecular and phenotypic data determined by the DLBCL90 assay and complete clinical information were available for all cases in that cohort.

Digital gene expression profiling

To extract RNA from the FFPE tissue samples, we used a Maxwell RSC RNA FFPE kit (Promega Corporation, Madison, WI) per the manufacturer's instructions. Gene expression profiling was performed on an nCounter platform (NanoString Technologies, Seattle, WA) using the DLBCL90 assay. The assay includes 30 genes to distinguish DLBCL from primary mediastinal B-cell lymphoma (previously reported as Lymph3Cx[17]), 15 genes to define COO (previously reported as Lymph2Cx[18]), and 30 to detect the DZ signature (1 overlapping with Lymph2Cx); additionally, there were 3 other important genes and 13 housekeeping genes. RNA (200 ng) extracted from FFPE tissues was hybridized overnight at 65°C with probes used to quantitate the 90 genes that contribute to the DLBCL90 assay, processed on the nCounter prep station, and analyzed with the nCounter digital analyzer to acquire gene expression data. The linear predictor score for COO was calculated as per previous reports,[11,18] and tumors were assigned to the GCB-DLBCL, ABC-DLBCL, or unclassified (UNC) DLBCL group. Based on the previous report that the COO classification had taken priority over the DZsig classification in ABC tumors, the DZsig scores were additionally examined in the GCB-DLBCL and UNC-DLBCL groups. DZsig-positive ($DZsig^{pos}$) tumors in the GCB-DLBCL and UNC-DLBCL groups were assigned to the $DZsig^{pos}$-DLBCL group, whereas DZsig-negative or DZsig-indeterminate tumors in the GCB-DLBCL and UNC-DLBCL groups were assigned to the GCB-DLBCL and UNC-DLBCL groups, respectively (Figure 1A).

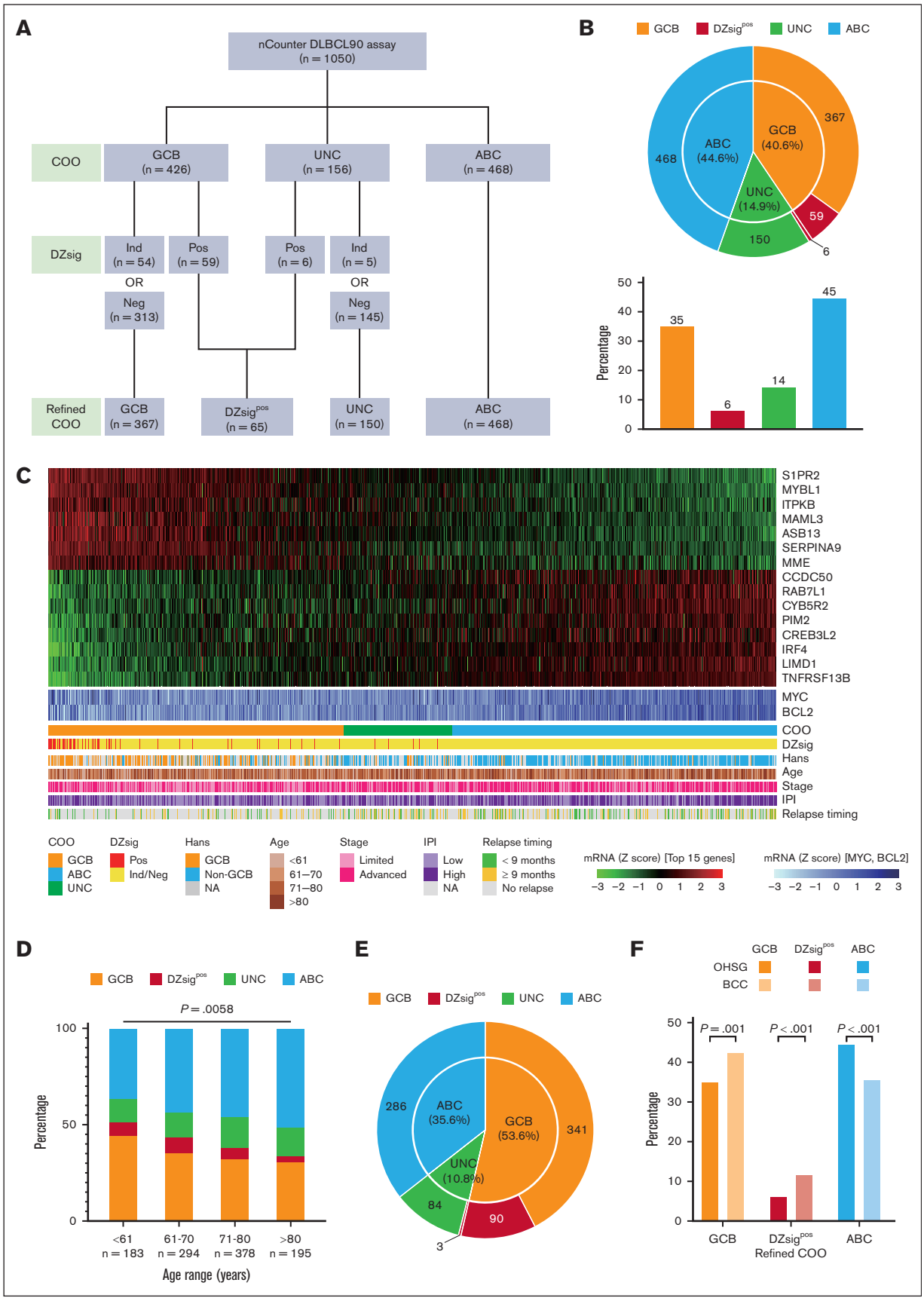
A
nCounter DLBCL90 assay (n = 1050)
COO
GCB (n = 426)
UNC (n = 156)
ABC (n = 468)
DZsig
Ind (n = 54)
Pos (n = 59)
Pos (n = 6)
Ind (n = 5)
OR
Neg (n = 313)
OR
Neg (n = 145)
Refined COO
GCB (n = 367)
DZsig pos (n = 65)
UNC (n = 150)
ABC (n = 468)
B
GCB
DZsig pos
UNC
ABC
367
GCB (40.6%)
ABC (44.6%)
468
UNC (14.9%)
59
150
6
Percentage
35
6
14
45
C
S1PR2
MYBL1
ITPKB
MAML3
ASB13
SERPINA9
MME
CCDC50
RAB7L1
CYB5R2
PIM2
CREB3L2
IRF4
LIMD1
TNFRSF13B
MYC
BCL2
COO
DZsig
Hans
Age
Stage
IPI
Relapse timing
COO
GCB
ABC
UNC
DZsig
Pos
Ind/Neg
Hans
GCB
Non-GCB
NA
Age
<61
61–70
71–80
>80
Stage
Limited
Advanced
IPI
Low
High
NA
Relapse timing
< 9 months
≥ 9 months
No relapse
mRNA (Z score) [Top 15 genes]
−3 −2 −1 0 1 2 3
mRNA (Z score) [MYC, BCL2]
−3 −2 −1 0 1 2 3
D
GCB
DZsig pos
UNC
ABC
P = .0058
Percentage
<61 n = 183
61-70 n = 294
71-80 n = 378
>80 n = 195
Age range (years)
E
GCB
DZsig pos
UNC
ABC
286
ABC (35.6%)
GCB (53.6%)
341
UNC (10.8%)
84
90
3
F
GCB
DZsig pos
ABC
OHSG
BCC
P = .001
P < .001
P < .001
Percentage
GCB
DZsig pos
Refined COO
ABC

Figure 1.

Table 1. Characteristics of patients in this study cohort, based on molecular subtypes

	GCB	DZsig^{pos}	ABC	UNC	*P* value	*P* value*	*P* value†
Number of patients	367	65	468	150			
Age, y (n, %)							
Median	70	70	73	73			
<61	81 (22.1)	13 (20)	67 (14.3)	22 (14.7)	.022	1	.027
≥61	286 (77.9)	52 (80)	401 (85.7)	128 (85.3)			
Sex (n, %)							
Male	197 (53.7)	43 (66.2)	266 (56.8)	85 (56.7)	.304	.467	1
Female	170 (46.3)	22 (33.8)	202 (43.2)	65 (43.3)			
Performance status (n, %)							
0-1	307 (84.3)	51 (79.7)	369 (80)	126 (85.1)	.205	1	.729
2-4	57 (15.7)	13 (20.3)	92 (20)	22 (14.9)			
NA	3	1	7	2			
Stage (n, %)							
I/II	199 (54.2)	28 (43.1)	184 (39.3)	62 (41.3)	< .001	.641	< .001
III/IV	168 (45.8)	37 (56.9)	284 (60.7)	88 (58.7)			
LDH level (n, %)							
Normal	182 (49.6)	17 (26.2)	139 (29.7)	61 (40.9)	< .001	.003	< .001
>ULN	185 (50.4)	48 (73.8)	329 (70.3)	88 (59.1)			
NA	0	0	0	1			
Extranodal sites (n, %)							
0-1	305 (83.1)	51 (78.5)	355 (75.9)	119 (79.3)	.085	1	.077
≥2	62 (16.9)	14 (21.5)	113 (24.1)	31 (20.7)			
IPI risk group (n, %)							
Low (0-1)	140 (38.5)	14 (21.9)	98 (21.3)	37 (25.5)	< .001	.092	< .001
Low-intermediate (2)	89 (24.5)	17 (26.6)	121 (26.2)	37 (25.5)			
High-intermediate (3)	74 (20.3)	20 (31.3)	117 (25.4)	42 (29)			
High (4-5)	61 (16.8)	13 (20.3)	125 (27.1)	29 (20)			
NA	3	1	7	5			

NA, not applicable; ULN, upper limit of normal.
**P* value is based on the comparison between GCB and DZsig^{pos} subtypes.
†*P* value is based on the comparison between GCB and ABC subtypes.

IHC and FISH analyses on tissue microarrays

FFPE tissues with sufficient material and tumor content were selected for tissue microarray (TMA) construction. IHC staining on the 4-μm slides of TMAs was performed for MYC, BCL2, BCL6, CD3, CD4, CD8, CD10, CD31, CD68, and MUM1 (antibodies are listed in supplemental Table 1) on the Bond Rx platform (Leica Biosystems, Wetzlar, Germany), and their digital scanning images were analyzed independently using the QuPath.[19] Each cell was predicted with a deep learning model implemented in QuPath (StarDist extension), and then the pseudodetections were filtered out based on their detection probability (<0.3) and nuclei size (>100 μm^2). For staining intensity, we manually set thresholds to apply 4 step scoring (from 0 to ≥3), and cases that scored ≥1 were labeled as positive. In addition, a more detailed expression range could be assessed by evaluating continuous measurements of H-score, a weighted scoring system ranging from 0 to 300, taking into account the percentage of tumor cells with staining intensities of 0, 1, 2, and ≥3. The H-score was calculated for tumor cell staining using the following formula: H-score = (% at 0) × 0 + (% at 1+) × 1 + (% at 2+) × 2 + (% at 3+) × 3, as described

Figure 1. Distribution of refined COO in Japanese patients with DLBCL. (A) Gene expression profiling–based molecular classification algorithm using the DLBCL90 assay. (B) The number of patients with COO classification (inner circle) and with DZsig classification separated into a new class (outer circle). For the latter, the overall distribution between classes is shown in the bar graph. (C) Heat map shows the Lymph2Cx component of the DLBCL90 assay with the 15 informative genes shown as rows, and all 1050 DLBCLs shown as columns. Arrayed below the heat map are clinical characteristics of the tumors. (D) Comparison of the distribution of molecular subtypes according to age group. Multinomial logistic regression *P* value (GCB vs ABC) is shown above the bar plot. (E) The number of patients in the BCC cohort, with COO classification (inner circle) and DZsig classification (outer circle) separated into new classes. (F) Bar plot showing the distribution of refined COO in the 2 cohorts compared using Fisher exact test. Ind, indeterminate; mRNA, messenger RNA; Neg, negative; OHSG, Okayama Hematology Study Group; Pos, positive.

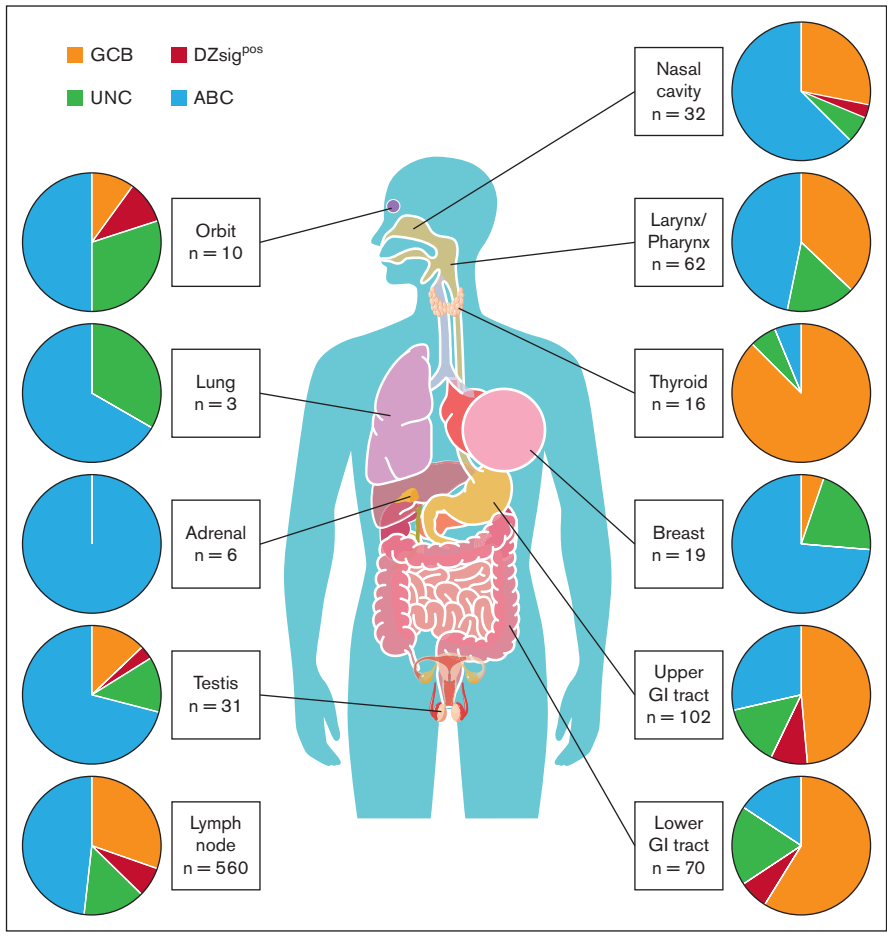

Figure 2. Distribution of molecular subtypes according to biopsy sites. Pie charts represent the frequency of molecular subtypes in each biopsy site.

previously.[20] The positive ratio for CD31 staining was calculated as the sum of all positive areas divided by the total area of each TMA core.

Fluorescence in situ hybridization (FISH) analysis was performed using commercially available dual-color, break-apart probes (probes are listed in supplemental Table 2). Two investigators (Y.N. and T.U.) independently scored at least 100 nuclei per tumor according to previous methods.[21-23] The tumors displaying break-apart signals in ≥10% of cells were considered to have translocation.

Statistical analysis

We used the Fisher exact test to compare categorical data. The Wilcoxon rank-sum test was used between 2 groups, whereas the Kruskal-Wallis test was used for multiple comparisons for nonparametric testing to compare numerical data. Bonferroni correction for multiple comparisons was applied when necessary. The Kaplan-Meier method was used to estimate progression-free survival (PFS; progression/relapse or death from any cause) and overall survival (OS; death from any cause), with the log-rank test performed to compare survival curves. Univariable and multivariable Cox proportional hazard regression models were used to evaluate potential prognostic factors. We used multinomial logistic regression to estimate odds ratios and 95% confidence intervals (CIs) to determine an association between age groups and molecular subtypes. We also performed logistic regression analyses to evaluate the associations of the COO distributions in our and BCC cohorts with clinical factors, including age. All reported P values are 2-sided, and those $<.05$ were considered statistically significant. All analyses were performed using R software version 4.2.1 (https://cran.r-project.org) and GraphPad Prism version 9.

Results

Determination of COO and the DZsig in Japanese patients with DLBCL

DLBCL90 was successfully performed in 1050 of 1576 patients. Of the 526 patients for whom a DLBCL90 result was not obtained, 298 did not have FFPE tissue samples available, 171 did not have sufficient RNA, and 57 did not meet the previously established quality criteria for DLBCL90 (supplemental Figure 1). The patient demographics and baseline characteristics of the final cohort are presented in supplemental Figure 2 and supplemental Tables 3 and 4. There were no significant differences in the baseline characteristics between the final study cohort and the excluded 526 cases, with the exception that biopsy specimens were more frequently obtained from extranodal sites in the excluded cases ($P < .001$). The median age was 72 years (range, 18-95); 591 of 1050 (56%) were men, and 481 of 1050 (46%) had a high or high-intermediate risk based on the international prognostic index (IPI).

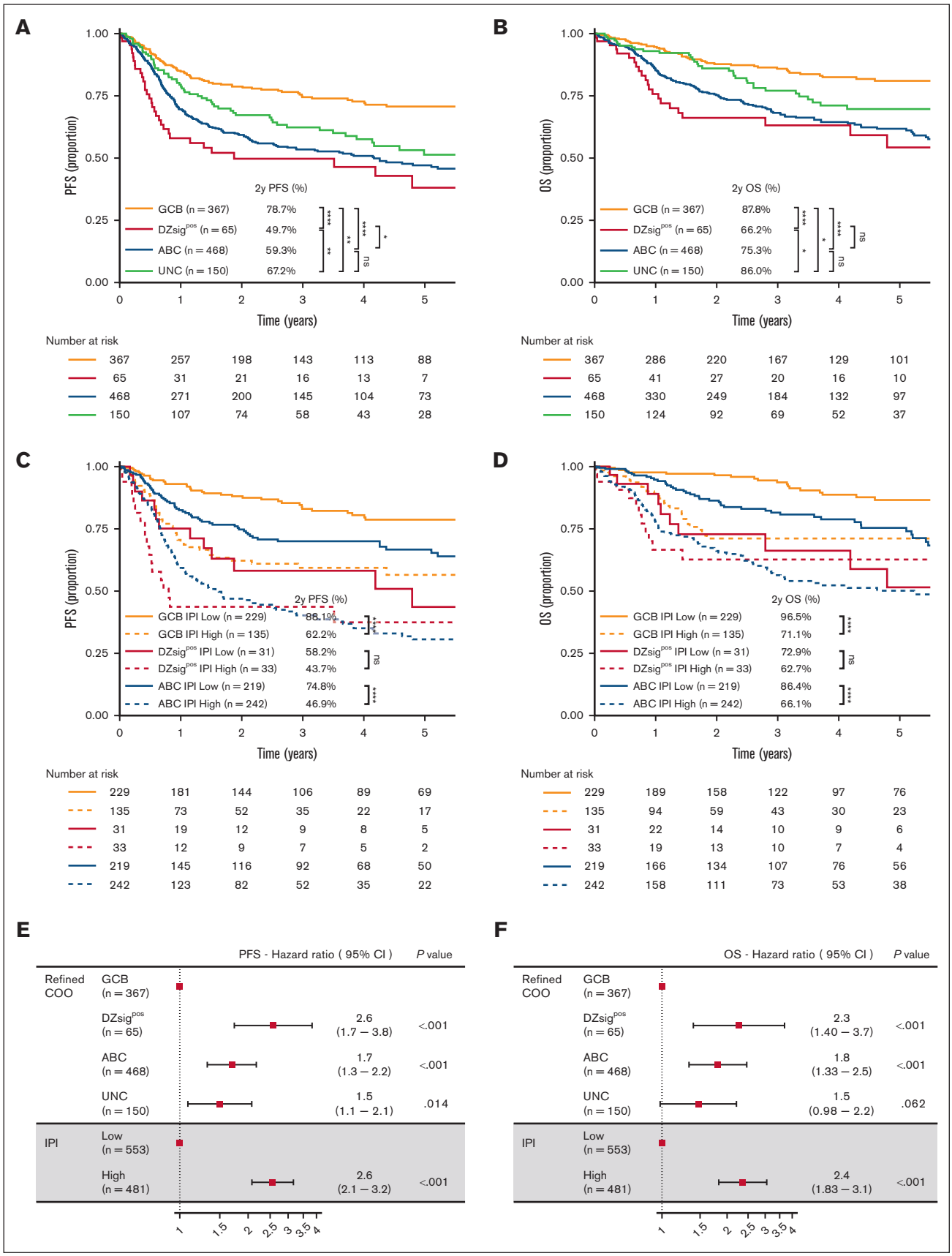
A
PFS (proportion)
Time (years)
2y PFS (%)
GCB (n = 367) 78.7%
DZsig^pos (n = 65) 49.7%
ABC (n = 468) 59.3%
UNC (n = 150) 67.2%
Number at risk
367 257 198 143 113 88
65 31 21 16 13 7
468 271 200 145 104 73
150 107 74 58 43 28
B
OS (proportion)
Time (years)
2y OS (%)
GCB (n = 367) 87.8%
DZsig^pos (n = 65) 66.2%
ABC (n = 468) 75.3%
UNC (n = 150) 86.0%
Number at risk
367 286 220 167 129 101
65 41 27 20 16 10
468 330 249 184 132 97
150 124 92 69 52 37
C
PFS (proportion)
Time (years)
2y PFS (%)
GCB IPI Low (n = 229) 88.1%
GCB IPI High (n = 135) 62.2%
DZsig^pos IPI Low (n = 31) 58.2%
DZsig^pos IPI High (n = 33) 43.7%
ABC IPI Low (n = 219) 74.8%
ABC IPI High (n = 242) 46.9%
Number at risk
229 181 144 106 89 69
135 73 52 35 22 17
31 19 12 9 8 5
33 12 9 7 5 2
219 145 116 92 68 50
242 123 82 52 35 22
D
OS (proportion)
Time (years)
2y OS (%)
GCB IPI Low (n = 229) 96.5%
GCB IPI High (n = 135) 71.1%
DZsig^pos IPI Low (n = 31) 72.9%
DZsig^pos IPI High (n = 33) 62.7%
ABC IPI Low (n = 219) 86.4%
ABC IPI High (n = 242) 66.1%
Number at risk
229 189 158 122 97 76
135 94 59 43 30 23
31 22 14 10 9 6
33 19 13 10 7 4
219 166 134 107 76 56
242 158 111 73 53 38
E
PFS - Hazard ratio (95% CI)
P value
Refined COO
GCB (n = 367)
DZsig^pos (n = 65) 2.6 (1.7 – 3.8) <.001
ABC (n = 468) 1.7 (1.3 – 2.2) <.001
UNC (n = 150) 1.5 (1.1 – 2.1) .014
IPI
Low (n = 553)
High (n = 481) 2.6 (2.1 – 3.2) <.001
F
OS - Hazard ratio (95% CI)
P value
Refined COO
GCB (n = 367)
DZsig^pos (n = 65) 2.3 (1.40 – 3.7) <.001
ABC (n = 468) 1.8 (1.33 – 2.5) <.001
UNC (n = 150) 1.5 (0.98 – 2.2) .062
IPI
Low (n = 553)
High (n = 481) 2.4 (1.83 – 3.1) <.001

Figure 3.

Of the 1050 patients, 426 (41%) had a COO of GCB, 468 (45%) had ABC, and 156 (15%) had UNC (Figure 1A-C). Within the GCB-DLBCL and UNC-DLBCL groups, 65 patients were assigned to the DZsig^{pos} group, and the remaining patients were assigned to their respective COO subgroups, per the algorithm shown in Figure 1A. As a result, patients in our cohort were assigned into 4 molecular subtypes as follows: 367 patients (35.0%) to GCB, 65 (6.2%) to DZsig^{pos}, 468 (44.6%) to ABC, and 150 (14.3%) to UNC (Figure 1A-C).

ABC-DLBCL was associated with unfavorable IPI factors for age, disease stage, and lactate dehydrogenase (LDH) levels compared with GCB-DLBCL ($P = .03$, $P < .001$, and $P < .001$, respectively). In contrast, there were no significant differences in the baseline characteristics between patients in the DZsig^{pos}-DLBCL and GCB-DLBCL groups, with the exception of elevated LDH ($P = .03$; Table 1). We also analyzed the association of molecular subtypes with age using the multinomial logistic regression method, which notably revealed that the proportion of patients with ABC-DLBCL was significantly increased in higher-age groups compared with that of patients with GCB-DLBCL ($P = .006$; Figure 1D).

Comparisons of the baseline characteristics of patients in this study with BCC real-world data showed that our cohort included patients with DLBCL who were significantly older and had a higher proportion of elevated LDH ($P < .001$; supplemental Table 5). In the BCC cohort (n = 804), there were 286 ABC-DLBCL, 341 GCB-DLBCL, 93 DZsig^{pos}-DLBCL, and 84 UNC-DLBCL cases (Figure 1E), with the proportion of patients with ABC-DLBCL being significantly higher (44.6% vs 35.6%) and those with GCB-DLBCL and DZsig^{pos}-DLBCL being significantly lower (35.0% vs 42.4% and 6.2% vs 11.6%, respectively) in the Japanese cohort (all $P < .01$ using Fisher exact test; Figure 1F). Based on the logistic regression models, our cohort was also found to have a statistically significant higher proportion of patients with ABC-DLBCL compared with the BCC cohort after adjusting for age and other IPI factors (supplemental Figure 3).

Association between biopsy sites and molecular subtypes

Half of the cases (490 of 1050) in this cohort were diagnosed using biopsy samples obtained from various extranodal sites (biopsy information of the excluded cohort is also shown in supplemental Table 4), prompting further analyses of the association of biopsy sites with molecular subtypes. The distribution of molecular subtypes based on biopsy sites is shown in Figure 2 and supplemental Figure 4. The proportions of ABC, GCB, and DZsig^{pos}-DLBCL in the nodal sites were 48.2% (270 of 560 cases), 30.4% (170 of 560 cases), and 7.0% (39 of 560 cases), respectively. When analyzing extranodal sites, ABC-DLBCL was enriched in the breast (73.7% [14 of 19 cases]; $P < .05$, Fisher exact test) and testis (71.0% [22 of 31 cases]; $P < .05$, Fisher exact test) compared with nodal sites, which is consistent with previous reports.[24,25] Remarkably, GCB-DLBCL tumors were significantly enriched in the upper and lower gastrointestinal (GI) tract (58.8% [60 of 102 cases] and 48.6% [34 of 70 cases], respectively; both $P < .01$, Fisher exact test) and thyroid gland (87.5% [14 of 16 cases]; $P < .01$, Fisher exact test) compared with nodal sites. In contrast, DZsig^{pos} tumors were not significantly enriched in any extranodal sites compared with nodal sites (Figure 2; supplemental Figure 4; supplemental Table 6). We also analyzed the associations between COO and biopsy sites in stage I/II (limited) and III/IV (advanced) groups separately and found similar trends in these 2 groups. Indeed, GCB-DLBCL was significantly enriched in biopsy specimen from the upper GI tract and thyroid, and ABC-DLBCL in the breast in limited disease (all, $P < .05$). Nonetheless, in limited disease, there was a trend toward the enrichment of GCB-DLBCL and ABC-DLBCL in the lower GI tract ($P = .12$) and testis ($P = .08$), respectively, probably not reaching statistical significance because of the small sample size (supplemental Figure 5).

Prognostic significance of the molecular subtypes in Japanese DLBCL

With a median follow-up of 2.8 years (range, 0.05-11) in living patients, the 2-year PFS and OS rates of the cohort were 66.6% (95% CI, 63.6-69.8) and 80.6% (95% CI, 78.0-83.3), respectively (supplemental Figure 2). The survival outcomes of the excluded cases were similar to those of the final cohort (supplemental Figure 2). Compared with GCB-DLBCL, patients with DZsig^{pos}-DLBCL and ABC-DLBCL had significantly shorter survival (log-rank, $P < .0001$ for PFS and OS; Figure 3A-B; supplemental Table 7). Indeed, DZsig^{pos}-DLBCL exhibited the poorest outcomes, with 2-year PFS and OS rates of 49.7% and 66.2%, respectively. In sharp contrast, GCB-DLBCL had excellent an OS rate of 88% at 2 years. The outcomes of DZsig-intermediate and DZsig-negative tumors were similar and significantly better than those of DZsig^{pos} tumors, indicating the clinical relevance of identifying DZsig^{pos}-DLBCL (supplemental Figure 6). It is noteworthy that both our study and the BCC study had similar outcomes for patients in each molecular subtype, except for the PFS in GCB (supplemental Figure 7), indicating that the molecular subtype had a similar significant prognostic impact in Japanese DLBCL, which is consistent with previous reports.[11,12,25] We also found that the proportion of primary refractory disease (refractory or relapse within 9 months of diagnosis) within all relapse/progressions was highest in DZsig^{pos}-DLBCL (68%) compared with other subtypes ($P = .046$; GCB-DLBCL, 44%; ABC-DLBCL, 49%; and UNC, 41%; supplemental Table 8).

In our cohort, patients with a high- or high-intermediate–risk IPI scores also had shorter survival than those with low- or low-intermediate–risk IPI scores (supplemental Figure 8; log-rank $P < .001$ for PFS and OS).

Within the molecular subtypes, IPI scores were significantly associated with outcomes in ABC-DLBCL and GCB-DLBCL ($P < .0001$ for PFS and OS in both subtypes but did not significantly stratify patients with DZsig^{pos}-DLBCL; Figure 3C-D; supplemental Figure 9). Multivariable analyses revealed that the DZsig^{pos} and

Figure 3. Prognostic significance of molecular classification of DLBCL. (A,B) Kaplan-Meier curves represent PFS and OS, per the molecular subtypes. (C,D) Kaplan-Meier curves showing OS according to the molecular subtypes combined with 2 IPI risk groups: low/low-intermediate–risk IPI group (low) and high/high-intermediate–risk IPI group (high). (E,F) Forest plots show the results of multivariable analyses (PFS and OS). IPI scores were classified into 2 groups as described earlier. DPE, dual protein expressor; ns, not significant; PR, primary refractory. *$P < .05$; **$P < .01$; ***$P < .001$; ****$P < .0001$.

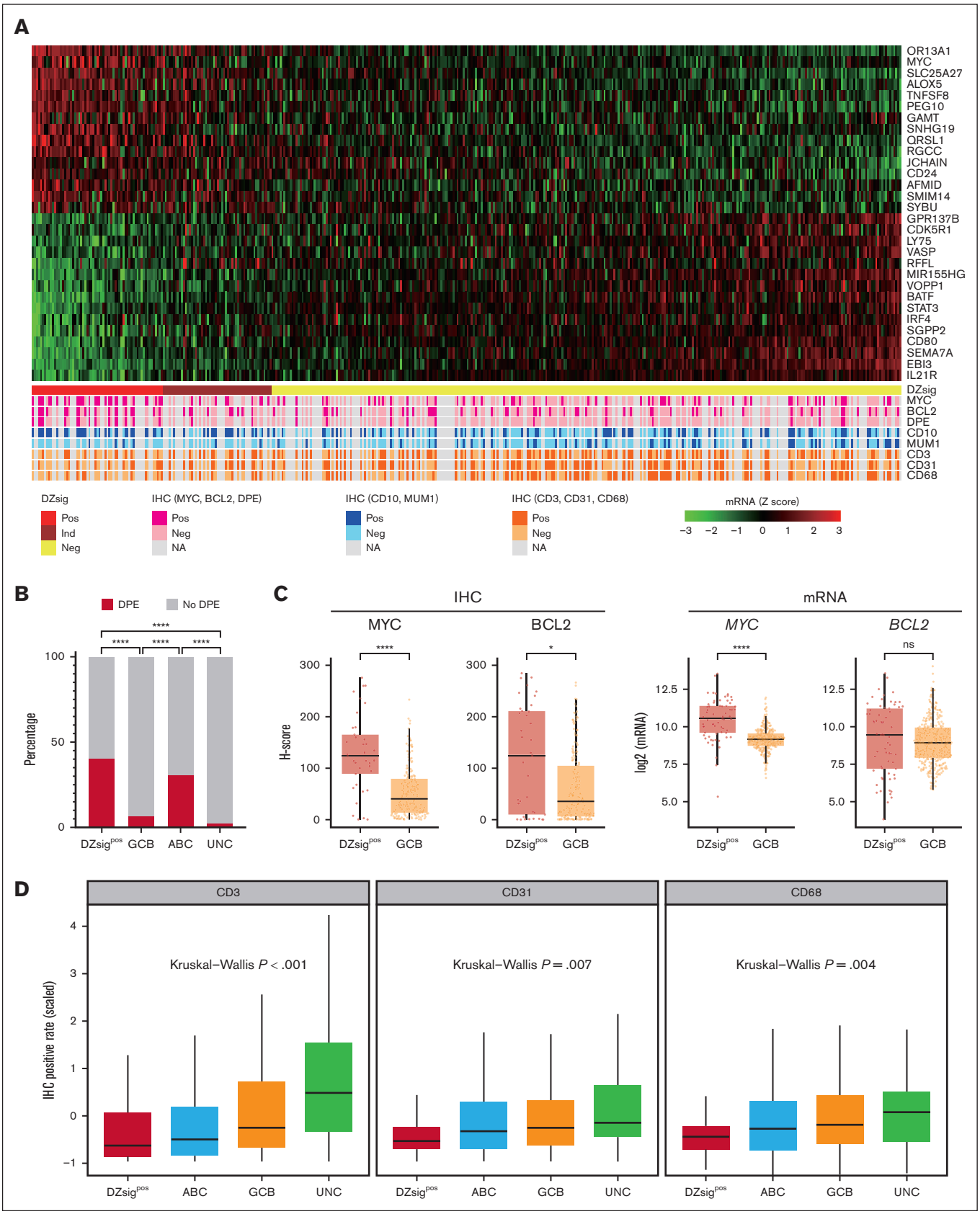
A
OR13A1
MYC
SLC25A27
ALOX5
TNFSF8
PEG10
GAMT
SNHG19
QRSL1
RGCC
JCHAIN
CD24
AFMID
SMIM14
SYBU
GPR137B
CDK5R1
LY75
VASP
RFFL
MIR155HG
VOPP1
BATF
STAT3
IRF4
SGPP2
CD80
SEMA7A
EBI3
IL21R
DZsig
MYC
BCL2
DPE
CD10
MUM1
CD3
CD31
CD68
DZsig
Pos
Ind
Neg
IHC (MYC, BCL2, DPE)
Pos
Neg
NA
IHC (CD10, MUM1)
Pos
Neg
NA
IHC (CD3, CD31, CD68)
Pos
Neg
NA
mRNA (Z score)
−3 −2 −1 0 1 2 3
B
DPE
No DPE
****
****
****
****
100
50
0
Percentage
DZsig^pos
GCB
ABC
UNC
C
IHC
MYC
BCL2
****
*
300
200
100
0
H-score
DZsig^pos
GCB
mRNA
MYC
BCL2
****
ns
12.5
10.0
7.5
5.0
log2 (mRNA)
DZsig^pos
GCB
D
CD3
CD31
CD68
Kruskal–Wallis P < .001
Kruskal–Wallis P = .007
Kruskal–Wallis P = .004
4
3
2
1
0
−1
IHC positive rate (scaled)
DZsig^pos
ABC
GCB
UNC

Figure 4.

ABC subtypes were independent predictors of PFS and OS when adjusted for the 2 IPI groups (Figure 3E-F). When stratified per the IPI group, the prognostic effect of the molecular subtypes was more evident in the low-risk IPI group (supplemental Figure 10).

Phenotypical characterization of the DZ signature

These results demonstrate the distinct clinical relevance of the DZsig, prompting us to further analyze the phenotypic characteristics associated with DZsig^{pos}-DLBCL. FISH analysis in 187 tumors showed that HGBL-DH-*BCL2* was detected in 4 of 9 DZsig^{pos}-DLBCL cases (44%), whereas only 2 of the remaining 178 tumors were HGBL-DH-*BCL2*. This is consistent with previous results,[11,12] albeit with lower sample size evaluated in this study (supplemental Figure 11). IHC studies indicated that patients with concurrent MYC and BCL2 expression (647 and 649 tumors available for MYC and BCL2, respectively) were found in 41% of cases with DZsig^{pos}-DLBCL, which was a significantly higher percentage than that of GCB-DLBCL (7%; $P < .0001$), shown in Figure 4A-B. Indeed, as determined by the H-score, DZsig^{pos} tumors had a significantly higher protein expression of MYC and BCL2 compared with GCB tumors ($P < .001$ and $P < .05$, respectively), whereas the messenger RNA expression of *MYC* ($P < .001$), but not that of *BCL2*, was significantly higher (Figure 4C). Because studies have demonstrated the critical role of the tumor microenvironment (TME) in understanding the biology and therapeutic targets of DLBCL,[26-29] we sought to characterize the TME of our DLBCL cohort and investigate its association with molecular subtypes and clinical outcomes. IHC staining revealed that the proportion of CD3^{+}, tumor-infiltrating lymphocytes was the lowest in patients with DZsig^{pos}-DLBCL, followed by ABC-DLBCL, GCB-DLBCL, and UNC-DLBCL in ascending order ($P < .001$, Kruskal-Wallis test), which is in line with the findings of previous studies.[11,26] Furthermore, the macrophage and microvessel densities, respectively defined by CD68 and CD31, were also decreased in DZsig^{pos}-DLBCL and ABC-DLBCL (both $P < .05$, Kruskal-Wallis test), indicating that the microenvironmental components were consistently depleted in these subtypes (Figure 4D).

Discussion

In this real-world study, we determined the distribution and clinical relevance of transcriptomic COO profiling, including DZsig, with the largest sample size in Asian countries, to our knowledge, demonstrating the high prevalence of ABC-DLBCL, which contrasts with Western countries, where GCB-DLBCL constitutes the majority of DLBCL.[11,18] This is in line with the results of 2 recent phase 3 trials,[30,31] wherein 51% to 62% of patients in Asian countries had the ABC subtype, compared with only 25% to 36% of patients in North America,[32,33] suggesting the importance of a geographical-based design and size estimation in clinical trials considering COO subtypes. Of note, ABC-DLBCL was still more prevalent in our cohort than in the BCC cohort after adjusting for age and other clinical factors. In the POLARIX study, which showed higher prevalence of ABC-DLBCL in Asian countries,[33] there was also no significant difference in the age and serum LDH level at baseline between Asian and global populations. Another study using a clinical trial data set, which also demonstrated the increased proportion of ABC-DLBCL in Asian populations, suggested the potential association with higher prevalence of Epstein-Barr virus positivity in Asian countries.[32] Taken together, the cause of the increased proportion of ABC-DLBCL in Asian populations needs to be elucidated. Furthermore, our study used the DLBCL90 assay, providing more comprehensive transcriptomic subtypes to distinguish DZsig^{pos}-DLBCL from GCB-DLBCL, which has a putative COO of the germinal center DZ.[11] In line with recent studies, the DZsig was significantly associated with poor prognosis and a lower representation of the TME in our cohort,[11,12,25,26] suggesting the clinical and biological significance of the DZsig regardless of the geographical region.

This study demonstrated that in patients undergoing R-CHOP immunochemotherapy, those with ABC-DLBCL and DZsig^{pos}-DLBCL have worse prognosis compared with patients with GCB-DLBCL. Recently, the novel immunotherapeutic drug polatuzumab vedotin, which is a potential replacement for vincristine (pola-R-CHP), showed a PFS benefit over the R-CHOP regimen in the phase 3 POLARIX study.[31] Remarkably, an exploratory subgroup analysis suggested a benefit with the pola-R-CHP regimen in patients with ABC-DLBCL, indicating that the clinical impact of pola-R-CHP might be greater in Japanese populations. However, the subgroup analyses were not sufficiently powered, and the DZsig was not available. Thus, future studies are warranted to assess the clinical significance of the refined COO classification in pola-R-CHP, which can help identify high-risk DLBCL populations requiring alternative treatment approaches.

To date, only a few studies have comprehensively determined the COO subtype of primary extranodal lymphomas.[25,34] Moreover, the biopsy sites were not clearly identified in these studies; thus, our data set, which contains detailed information regarding the biopsies, could be used to assess the COO profile according to the disease site. Consistent with previous reports,[24,35,36] ABC-DLBCL was more commonly observed in cases with biopsy samples obtained from the testis, breast, and adrenal gland. Notably, GCB-DLBCL was significantly enriched in biopsy samples from the thyroid gland and both upper and lower GI tracts compared with those from the lymph node. The associations of GCB-DLBCL with the GI and thyroid biopsies were also observed in cases with limited-stage disease, indicating that GCB-DLBCL are common in primary GI tract and thyroid lymphomas. Some low-grade lymphomas, such as marginal zone lymphoma in the thyroid and duodenal follicular lymphoma, are known to arise in these organs, indicating the possibility that these DLBCL arise from occult low-grade lymphomas. In contrast, our results did not show the specific extranodal sites involving DZsig^{pos} tumors, probably because of the small number of DZsig^{pos} cases that we included in our study.

There is increasing evidence that interactions between cell-intrinsic changes and host immune response of DLBCL tumors are critical

Figure 4. Phenotypic characterization of the DZsig. (A) Heat map represents the 30 informative DZsig genes shown as rows, and the 432 patients with GCB or DZsig^{pos}-DLBCLs shown as columns. Arrayed below the heat map are immunohistochemical characteristics of the tumors. (B) Bar plots show the proportion of MYC/BCL2 DPEs, per molecular subtypes. (C) Box plots showing H-score (left) of c-MYC and BCL2, and messenger RNA expression (right) of *MYC* and *BCL2* in DZsig^{pos} tumors vs GCB tumors, compared using Wilcoxon rank-sum test. (D) Comparison of mean z scores of IHC-positive rate for each antibody per molecular subtypes. mRNA, messenger RNA.

for disease development.[26-29,37-39] In particular, the disrupted cross talk between lymphoma cells and the microenvironment contribute to escaping immune surveillance, and genetic and epigenetic alterations are suggested as biological mechanisms of immune escape.[25,37-39] Notably, DZsig^{pos} and molecular high-grade subtypes were characterized with an overall lower presence of the microenvironment, including stromal components, indicating the strong cell-autonomous mechanism underlying aggressive clinical behavior.[11,12,26] Our work not only validates such biological aspects of high-risk DLBCL groups but also suggests the clinical utility, based on an IHC method, in the evaluation of the TME and response to treatment, particularly, immunomodulatory and cellular therapies.

There were some limitations inherent to the retrospective nature of this study. Cases with insufficient RNA or unavailable FFPE tissue samples were excluded, mainly because of limited access to biopsies from extranodal sites. Although the survival outcomes of the excluded cases did not differ significantly from those of the final cohort, they potentially affected the distribution and clinical significance of COO subtypes in our cohort. Another potential selection bias is that some patients who received intensive treatment regimens were excluded; this group of patients would often include patients with HGBL-DH-*BCL2*. This might also have excluded patients with DZsig^{pos}-DLBCL, which resulted in the underestimation of this molecular subtype in our cohort.

In conclusion, to our knowledge, this study is the first to evaluate the clinical relevance of molecular classifications, including the DZ signature, outside Western countries. Our results demonstrated a high prevalence of ABC-DLBCL, which underlines the need for adjustments in study design and caution when interpreting the results of clinical trials. Furthermore, we provided a more comprehensive analysis of transcriptomic subtypes to distinguish DZsig^{pos}-DLBCL from GCB-DLBCL, demonstrating the clinical and biological significance of the DZ signature regardless of geographical region. In addition to being able to determine the unfavorable prognosis of patients with DLBCL who may need alternative treatment approaches, the absence of the DZsig also identifies the GCB-DLBCL subgroup as having excellent outcomes after R-CHOP therapy. Our IHC studies also showed a lower involvement of the TME in DZsig^{pos} tumors, which is in line with the findings of previous transcriptomic analyses.[11,12,26] Thus, these consistent clinical and biological findings may further advance the recognition of the DZsig and the refined COO classification. The robustness of DLBCL90, which can identify patients who are more likely to benefit from intensified treatment and novel therapies, should be evaluated in future prospective trials.

Acknowledgments

The authors thank Yuka Gion, Misa Sakamoto, Yuria Egusa, Azusa Fujita, Jin Kiyama, Yukina Maekawa, Sayako Yoshida, and Kanna Maehama for the histology expertise in FFPE block processing and tissue microarray construction. The authors also thank Kumiko Ohsawa, Takehiro Matsubara, and Yukari Kawai for expert technical assistance.

This work was supported by the Japan Agency for Medical Research and Development (JP20cm0106471h0001).

Authorship

Contribution: T.U. and D.E. designed and performed the research, analyzed and interpreted data, and wrote the manuscript; K. Sunami, T.I., Y. Nawa, Y.H., K.Y., S.F., I.Y., T. Yano, A.Y., T.K., H.F., N.A., H.N., K.F., N.F., and K.-i.M. provided clinical data; K. Sawada, S.M., J.-i.T., A.N., Y.S., and T. Yoshino performed pathological experiments and review; T.U., Y. Naoi, A.J., M.B., R.C., H.M., K.I., H.K., K.T., H.U., H.I., and S.T. performed experiments and analyzed data; and Y.M., D.W.S., and D.E. reviewed the manuscript.

Conflict-of-interest disclosure: K. Sunami declares research funding and honoraria from Celgene, Sanofi, Bristol Myers Squibb (BMS), Ono, and Janssen, and research funding from Takeda, AbbVie, GlaxoSmithKline, Chugai, Otsuka, Merck Sharp and Dohme, Novartis, Astellas Amgen, Pfizer, Parexel, Kyowa Kirin, Symbio, and Agios. I.Y. declares research funding and honoraria from Kyowa Kirin and Chugai, and honoraria from Eisai, Janssen, Nippon-Shinyaku, Otsuka, Symbio, Takeda, Sumitomo Pharma, and Meiji. N.A. received honoraria from AbbVie. N.F. received honoraria from Novartis, Daiichi Sankyo, Chugai, Astellas, Janssen, and BMS. J.-i.T. declares research funding, honoraria, and speakers' bureau fees from Takeda; honoraria and speakers, bureau fees from Chugai and BMS; and research funding from Nichirei and Ridgelinez. Y.M. declares research funding and scholarship donations from Chugai; research funding from Nippon Shinyaku; and scholarship donations from Eisai, Otsuka, Kyowa Kirin, and Takeda. D.W.S. declares consultancy for AbbVie and Incyte; consultancy for and honoraria from AstraZeneca; consultancy for and research funding from Janssen; research funding from Roche; and patent with NanoString. D.E. declares research funding from Nippon Shinyaku; honoraria from Eisai and Kyowa Kirin; and research funding and honoraria from Chugai. The remaining authors declare no competing financial interests.

ORCID profiles: T.U., 0000-0002-1718-7110; R.C., 0000-0002-3125-4818; H.K., 0000-0001-7892-4674; A.Y., 0000-0001-7574-6446; T.K., 0000-0002-6395-7913; H.N., 0000-0003-1649-4642; N.F., 0000-0002-8043-7768; K.S., 0000-0002-6357-9473; S.M., 0000-0003-3986-1409; A.N., 0000-0003-1485-0527; Y.S., 0000-0001-5234-6861; D.W.S., 0000-0002-0435-5947.

Correspondence: Daisuke Ennishi, Center for Comprehensive Genomic Medicine, Okayama University Hospital, Okayama, Japan 700-8558, Japan; email: daisukeennishi@okayama-u.ac.jp.

References

1. Alizadeh AA, Eisen MB, Davis RE, et al. Distinct types of diffuse large B-cell lymphoma identified by gene expression profiling. *Nature*. 2000;403(6769):503-511.

2. Lenz G, Wright G, Dave SS, et al. Stromal gene signatures in large-B-cell lymphomas. *N Engl J Med*. 2008;359(22):2313-2323.

3. Shipp MA, Ross KN, Tamayo P, et al. Diffuse large B-cell lymphoma outcome prediction by gene-expression profiling and supervised machine learning. *Nat Med*. 2002;8(1):68-74.
4. Hans CP, Weisenburger DD, Greiner TC, et al. Confirmation of the molecular classification of diffuse large B-cell lymphoma by immunohistochemistry using a tissue microarray. *Blood*. 2004;103(1):275-282.
5. Choi WW, Weisenburger DD, Greiner TC, et al. A new immunostain algorithm classifies diffuse large B-cell lymphoma into molecular subtypes with high accuracy. *Clin Cancer Res*. 2009;15(17):5494-5502.
6. Meyer PN, Fu K, Greiner TC, et al. Immunohistochemical methods for predicting cell of origin and survival in patients with diffuse large B-cell lymphoma treated with rituximab. *J Clin Oncol*. 2011;29(2):200-207.
7. Visco C, Li Y, Xu-Monette ZY, et al. Comprehensive gene expression profiling and immunohistochemical studies support application of immunophenotypic algorithm for molecular subtype classification in diffuse large B-cell lymphoma: a report from the International DLBCL Rituximab-CHOP Consortium Program Study. *Leukemia*. 2012;26(9):2103-2113.
8. Coutinho R, Clear AJ, Owen A, et al. Poor concordance among nine immunohistochemistry classifiers of cell-of-origin for diffuse large B-cell lymphoma: implications for therapeutic strategies. *Clin Cancer Res*. 2013;19(24):6686-6695.
9. Gutierrez-Garcia G, Cardesa-Salzmann T, Climent F, et al. Gene-expression profiling and not immunophenotypic algorithms predicts prognosis in patients with diffuse large B-cell lymphoma treated with immunochemotherapy. *Blood*. 2011;117(18):4836-4843.
10. Read JA, Koff JL, Nastoupil LJ, Williams JN, Cohen JB, Flowers CR. Evaluating cell-of-origin subtype methods for predicting diffuse large B-cell lymphoma survival: a meta-analysis of gene expression profiling and immunohistochemistry algorithms. *Clin Lymphoma Myeloma Leuk*. 2014;14(6):460-467.e2.
11. Ennishi D, Jiang A, Boyle M, et al. Double-hit gene expression signature defines a distinct subgroup of germinal center B-cell-like diffuse large B-cell lymphoma. *J Clin Oncol*. 2019;37(3):190-201.
12. Sha C, Barrans S, Cucco F, et al. Molecular high-grade B-cell lymphoma: defining a poor-risk group that requires different approaches to therapy. *J Clin Oncol*. 2019;37(3):202-212.
13. Holmes AB, Corinaldesi C, Shen Q, et al. Single-cell analysis of germinal-center B cells informs on lymphoma cell of origin and outcome. *J Exp Med*. 2020;217(10):e20200483.
14. Song JY, Perry AM, Herrera AF, et al. Double-hit signature with TP53 abnormalities predicts poor survival in patients with germinal center type diffuse large B-cell lymphoma treated with R-CHOP. *Clin Cancer Res*. 2021;27(6):1671-1680.
15. Alduaij W, Collinge B, Ben-Neriah S, et al. Molecular determinants of clinical outcomes in a real-world diffuse large B-cell lymphoma population. *Blood*. 2023;141(20):2493-2507.
16. Swerdlow SH, Campo E, Harris NL, et al. *WHO Classification of Tumours of Haematopoietic and Lymphoid Tissues*. Revised 4th ed. International Agency for Research on Cancer; 2017.
17. Mottok A, Wright G, Rosenwald A, et al. Molecular classification of primary mediastinal large B-cell lymphoma using routinely available tissue specimens. *Blood*. 2018;132(22):2401-2405.
18. Scott DW, Wright GW, Williams PM, et al. Determining cell-of-origin subtypes of diffuse large B-cell lymphoma using gene expression in formalin-fixed paraffin-embedded tissue. *Blood*. 2014;123(8):1214-1217.
19. Bankhead P, Loughrey MB, Fernandez JA, et al. QuPath: open source software for digital pathology image analysis. *Sci Rep*. 2017;7(1):16878.
20. Sehn LH, Herrera AF, Flowers CR, et al. Polatuzumab vedotin in relapsed or refractory diffuse large B-cell lymphoma. *J Clin Oncol*. 2020;38(2):155-165.
21. Copie-Bergman C, Gaulard P, Leroy K, et al. Immuno-fluorescence in situ hybridization index predicts survival in patients with diffuse large B-cell lymphoma treated with R-CHOP: a GELA study. *J Clin Oncol*. 2009;27(33):5573-5579.
22. Pedersen MO, Gang AO, Poulsen TS, et al. MYC translocation partner gene determines survival of patients with large B-cell lymphoma with MYC- or double-hit MYC/BCL2 translocations. *Eur J Haematol*. 2014;92(1):42-48.
23. Ennishi D, Mottok A, Ben-Neriah S, et al. Genetic profiling of MYC and BCL2 in diffuse large B-cell lymphoma determines cell-of-origin-specific clinical impact. *Blood*. 2017;129(20):2760-2770.
24. Deng L, Xu-Monette ZY, Loghavi S, et al. Primary testicular diffuse large B-cell lymphoma displays distinct clinical and biological features for treatment failure in rituximab era: a report from the International PTL Consortium. *Leukemia*. 2016;30(2):361-372.
25. Wright GW, Huang DW, Phelan JD, et al. A probabilistic classification tool for genetic subtypes of diffuse large B cell lymphoma with therapeutic implications. *Cancer Cell*. 2020;37(4):551-568.e14.
26. Kotlov N, Bagaev A, Revuelta MV, et al. Clinical and biological subtypes of B-cell lymphoma revealed by microenvironmental signatures. *Cancer Discov*. 2021;11(6):1468-1489.
27. Ennishi D, Takata K, Beguelin W, et al. Molecular and genetic characterization of MHC deficiency identifies EZH2 as therapeutic target for enhancing immune recognition. *Cancer Discov*. 2019;9(4):546-563.
28. Ennishi D, Healy S, Bashashati A, et al. TMEM30A loss-of-function mutations drive lymphomagenesis and confer therapeutically exploitable vulnerability in B-cell lymphoma. *Nat Med*. 2020;26(4):577-588.
29. Croci GA, Au-Yeung RKH, Reinke S, et al. SPARC-positive macrophages are the superior prognostic factor in the microenvironment of diffuse large B-cell lymphoma and independent of MYC rearrangement and double-/triple-hit status. *Ann Oncol*. 2021;32(11):1400-1409.

30. Nowakowski GS, Chiappella A, Witzig TE, et al. ROBUST: lenalidomide-R-CHOP versus placebo-R-CHOP in previously untreated ABC-type diffuse large B-cell lymphoma. *Future Oncol*. 2016;12(13):1553-1563.
31. Tilly H, Morschhauser F, Sehn LH, et al. Polatuzumab vedotin in previously untreated diffuse large B-cell lymphoma. *N Engl J Med*. 2022;386(4):351-363.
32. Nowakowski GS, Chiappella A, Witzig TE, et al. Variable global distribution of cell-of-origin from the ROBUST phase III study in diffuse large B-cell lymphoma. *Haematologica*. 2020;105(2):e72-e75.
33. Song Y, Tilly H, Rai S, et al. Polatuzumab vedotin in previously untreated DLBCL: an Asia subpopulation analysis from the phase 3 POLARIX trial. *Blood*. 2023;141(16):1971-1981.
34. Lopez-Guillermo A, Colomo L, Jimenez M, et al. Diffuse large B-cell lymphoma: clinical and biological characterization and outcome according to the nodal or extranodal primary origin. *J Clin Oncol*. 2005;23(12):2797-2804.
35. Twa DDW, Lee DG, Tan KL, et al. Genomic predictors of central nervous system relapse in primary testicular diffuse large B-cell lymphoma. *Blood*. 2021;137(9):1256-1259.
36. Taniguchi K, Takata K, Chuang SS, et al. Frequent MYD88 L265P and CD79B mutations in primary breast diffuse large B-cell lymphoma. *Am J Surg Pathol*. 2016;40(3):324-334.
37. Ennishi D, Hsi ED, Steidl C, Scott DW. Toward a new molecular taxonomy of diffuse large B-cell lymphoma. *Cancer Discov*. 2020;10(9):1267-1281.
38. Dersh D, Phelan JD, Gumina ME, et al. Genome-wide screens identify lineage- and tumor-specific genes modulating MHC-I- and MHC-II-restricted immunosurveillance of human lymphomas. *Immunity*. 2021;54(1):116-131.e10.
39. Fangazio M, Ladewig E, Gomez K, et al. Genetic mechanisms of HLA-I loss and immune escape in diffuse large B cell lymphoma. *Proc Natl Acad Sci U S A*. 2021;118(22):e2104504118.